Theor Chem Acc (2001) 106: 287–296
DOI 10.1007/s002140100276

Theoretical
Chemistry Accounts

Regular article

Rydberg character of the higher excited states of free-base porphin

Shigeyoshi Yamamoto[1], **Hiroshi Tatewaki**[2], **Osamu Kitao**[3], **Geerd H.F. Diercksen**[4]

[1] Faculty of Liberal Arts, Chukyo University, 101–2 Yagoto-Honmachi, Showa-ku, Nagoya 466-8666, Japan
[2] Institute of Natural Sciences, Nagoya City University, Aichi 467-8501, Japan
[3] National Institute of Materials and Chemical Research, Tsukuba, Ibaraki 305-8565 Japan,
Graduate School of Engineering, the University of Tokyo, 7-3-1 Hongo, Bunkyo-ku, Tokyo 113–8565, Japan
[4] Max-Planck-Institut für Astrophysik, Karl-Schwarzschild-Strasse 1, 85740 Garching, Germany

Received: 27 November 2000 / Accepted: 11 April 2001 / Published online: 27 June 2001

Abstract. The Rydberg character of the excited states of free-base porphin (FBP) has been investigated by the ab initio configuration interaction singles (CIS) method and the state-averaged complete-active-space self-consistent-field method. Double-zeta basis sets augmented with s, p, and d Rydberg functions and d polarization functions have been employed. Two types of molecular orbitals sets, the restricted Hartree–Fock molecular orbitals obtained for the ground state (^1A_g) and for the cation state (^2A_u), have been used in the CIS calculations. All the calculations show that Rydberg-type excitations play important roles especially in the N bands. In this article we propose applying the model of a perturbed Rydberg series to interpret the excited states of FBP. By using this model, we have succeeded in analyzing the characteristics of the excited states as well as the experimental oscillator strengths, which have considerable magnitude even in the higher excited states.

Key words: Free-base porphin – Rydberg character – Perturber – Excited state – Configuration interaction

1 Introduction

Free-base porphin (FBP) is the basic skeleton of various porphyrin compounds, derivatives of which play important roles especially in biological systems (hemoglobin, peroxidase P-450, cytochrome, etc.). The theoretical study of the electronic structure of the excited states of FBP is important in order to reveal the mechanism of the chemical reactions involving porphyrin, such as photosynthesis, as well as to assign their absorption spectra [1, 2]. The lowest excited states are the so-called Q and B (Soret) bands and they have been studied extensively experimentally and theoretically. The pioneering work is due to Gouterman [2], who explained the electronic structure of these bands by applying the four-orbital model.

Recent advances of computational methodology in quantum chemistry and of computer technology have made it possible to calculate the excited states of FBP reliably. Among them, the lowest two excited states, i.e., the Q and B bands, have been investigated extensively by many researchers. Some of the studies have been carried out using semiempirical theory [2–4] and others using ab initio methods, i.e., multireference configuration interaction singles and doubles (MRCISD) [5, 6], CI singles (CIS) [7, 8], second-order perturbation theory with a complete-active-space self-consistent-field reference function [9, 10], symmetry-adapted cluster CI [11–14], similarity-transformed equation-of-motion coupled cluster [15, 16], multireference Møller–Plessett perturbation theory [17], and multireference second-order perturbation theory (MRPT2) [18]. Computational studies of time-dependent density functional theory have also been published [19].

The spectral assignments given so far are summarized in Table 1. The Q and B bands can be characterized essentially by Gouterman's four-orbital model [2]. In fact, assignments due to theoretical studies are not contradictory to the four-orbital model. The only exception is the assignment by Nakatsuji et al. [11] of the second $^1B_{2u}$ state to the N bands rather than to the B bands.

There are N, L, and M bands above the B bands. For these states, a clear characterization has not been established yet. The diamond symbols in Table 1 indicate that the calculated oscillator strengths of the N bands are too large compared to the experimental value (below 0.1). All previous computational investigations have failed to give acceptable oscillator strengths for the N bands. Moreover, one can also find from Table 1 that the assignment of the L bands differs completely among the previous theoretical studies. Accordingly, there is no

Correspondence to: H. Tatewaki
e-mail: htatewak@nsc.nagoya-cu.ac.jp

Table 1. Previous studies on the excited states of free-base porphin (*FBP*). Excitation energies are in electron volts. Oscillator strengths are given in *parentheses*. *Diamond symbols* denote large discrepancy of the oscillator strength between experiment and calculation. Methods: symmetry-adapted cluster configuration interaction (*SAC-CI*); similarity-transformed equation-of-motion coupled cluster (*STEOM-CC*); second-order perturbation theory with a complete-active-space self-consistent-field reference function (*CASPT2*); time-dependent density functional theory (*TD-DFT*)

Experiment[a]	Method/Rydberg function[b]					
	SAC-CI[c] None	STEOM-CC None[d]	2s,2p[e]	CASPT2[f] None	SAC-CI[g] 2d	TD-DFT[h] None
	1-$^1B_{3u}$	1−$^1B_{3u}$	1−$^1B_{3u}$	1−$^1B_{3u}$	1−$^1B_{3u}$	1-$^1B_{3u}$
1.98Q_x	1.75	1.75	1.70	1.63	1.81	2.16
(0.01)	(0.00113)	(0.0007)	(–)	(0.004)	(0.00276)	(0.01)
	1-$^1B_{2u}$	1-$^1B_{2u}$	1-$^1B_{2u}$	1-$^1B_{2u}$	1-$^1B_{2u}$	1-$^1B_{2u}$
2.42Q_y	2.23	2.40	2.59	2.11	2.10	2.29
(0.06)	(0.00566)	(0.013)	(0.017)	(0.002)	(0.0163)	(0.0005)
	2-$^1B_{3u}$	2-$^1B_{3u}$	2-$^1B_{3u}$	2-$^1B_{2u}$	2-$^1B_{3u}$	2-$^1B_{3u}$
3.33B	3.56	3.47	3.63	3.08	3.47	2.98
(1.15)	(1.03)	(0.693)	(0.981)	(0.911)	(0.901)	(0.1338)
		2-$^1B_{2u}$	2-$^1B_{2u}$	2-$^1B_{3u}$	2-$^1B_{2u}$	2-$^1B_{2u}$
		3.62	3.74	3.12	3.69	3.01
		(1.20)	(1.37)	(0.704)	(1.88)	(0.04)
	2-$^1B_{2u}$	3-$^1B_{3u}$	3-$^1B_{3u}$	3-$^1B_{2u}$	3-$^1B_{3u}$	3-$^1B_{2u}$
3.65N	3.75	4.06	4.22	3.42	4.23	3.41
(< 0.1)	(1.73) ◆	(0.931)◆	(0.741)◆	(0.458)◆	(1.63) ◆	(0.8962) ◆
				3-$^1B_{3u}$	3-$^1B_{2u}$	3-$^1B_{2u}$
				3.53	4.40	3.47
				(0.833) ◆	(0.578) ◆	(0.7293) ◆
	3-$^1B_{3u}$	3-$^1B_{2u}$	3-$^1B_{2u}$	4-$^1B_{2u}$		4-$^1B_{3u}$
4.25L	4.24	4.35	4.63	3.96		3.76
(≈0.1)	(0.976)	(0.422)	(0.444)	(0.341)		(0.1272)
				4-$^1B_{3u}$		4-$^1B_{2u}$
				4.04		(3.77)
				(0.202)		(0.1688)
	3-$^1B_{2u}$	4-$^1B_{2u}$	4-$^1B_{2u}$			
4.67L	4.52	5.00	5.22			
(≈0.1)	(0.350)	(0.153)	(0.182)			
	4-$^1B_{2u}$	4-$^1B_{3u}$				
5.50M	5.31	5.17				
(≈0.3)	(0.280)	(0.272)				
	4-$^1B_{3u}$					
	5.45					
	(0.351)					

[a] Ref. [1]
[b] Entry "none" means that no Rydberg basis functions are used
[c] Entry title SAC-CI(B) in Table IV of Ref. [11]
[d] Entry title D_{4h} polarized in Table VII of Ref. [16]
[e] Entry title D_{4h} diffuse in Table III of Ref. [16]. Rydberg functions at the molecular center and at the pyrrole centers are used
[f] Ref. [10]
[g] Ref. [14]. Rydberg functions at the molecular center are used
[h] Ref. [19]

agreement about the character of these higher excited states.

We consider the discrepancy of the oscillator strengths of the N bands between the calculations and the experiments to be due to the mixing of valence- and Rydberg-type excitations, namely, a perturbed Rydberg series [20]. A perturbed Rydberg series is represented by the following equation as exemplified by Tatewaki [20] for the silicon atom,

$$\Phi'_{i\mathrm{R}} = C_{i\mathrm{v}}\phi_{\mathrm{v}} + \left(C_{ii}\phi_{i\mathrm{R}} + \sum_{n(n\neq i)} C_{in}\phi_{n\mathrm{R}} \right) , \qquad (1)$$

where ϕ_{v} is a valence configuration state function (CSF) and $\phi_{i\mathrm{R}}$ is obtained by diagonalizing the Hamiltonian matrix composed of Rydberg-type configurations.

$$H\phi_{i\mathrm{R}} = \varepsilon_{i\mathrm{R}}\phi_{i\mathrm{R}} \qquad (2)$$

In Eq. (1) we symbolically represent the valance state by only one term (ϕ_{v}). Tatewaki [20] showed that the valence-type configuration $3s3p^3$ strongly perturbs the $3s^2 3pnd$ ($n = 3$–13) $^3D^0$ Rydberg series of the silicon atom. In the lowest root of the CI calculation, the weights of the $3s^2 3p3d$ and that of $3s3p^3$ are 25.61 and 55.53%, respectively; however, in the second root, they are 70.16 and 11.43%, respectively. In the third root, the weights of the $3s^2 3p4d$ and that of $3s3p^3$ are 80.74 and 3.82%, respectively. We note that the sum of the weights of the perturber and the main Rydberg configurations are around 80% and the remaining contributions (20%) comes from Rydberg-type configurations other than the main one. It is thus essential that the different Rydberg states of the same symmetry are mixed through ϕ_{v} and the state $\Phi'_{i\mathrm{R}}$ has considerable oscillator strength even for large i. As seen from Table 1, the oscillator strength of 3.65N is less than 0.1, but the strengths are 0.1, 0.1,

and 0.3 for 4.25L, 4.67L, and 5.50M, respectively. This suggests that the higher FBP spectra consist of a perturbed Rydberg series. It is inferred that a valence-type configuration plays a role of the strong perturber for the N bands of FBP. No one has given such a view so far.

As shown in Table 1, some ab initio calculations were performed with Rydberg basis functions. Gwaltney and Bartlett [16] used s and p Rydberg functions at the molecular center and at the pyrrole centers. Tokita et al. [13] used s and p Rydberg functions on the nitrogen atoms. Kitao et al. [14] used d Rydberg functions at the molecular center. However, we consider that these functions are still insufficient for describing the Rydberg character of the excited states and that at least a p Rydberg function and a d polarization function have to be used on each heavy atom (carbon, nitrogen). Thus, we performed ab initio CIS and state-averaged complete-active-space self-consistent-field (sa-CASSCF) [21] calculations of the excited states of FBP with Rydberg functions and polarization functions.

We mainly focus on the higher excited states with transitions from the ground state, especially the $^1B_{3u}$ and $^1B_{2u}$ states, and try to analyze these states by the model of a perturbed Rydberg series.

2 Computational methods

The idealized X-ray structure of FBP ($C_{20}N_4H_{14}$) was introduced by Sekino and Kobayashi [22] and has been used by other researchers [11, 13, 15]. We have adopted this structure in the present study. Following the customary way shown in Fig. 1a, we placed the FBP molecule on the *xy*-plane and the inner two hydrogen atoms on the *x*-axis. Without the inner hydrogen atoms the molecule satisfies D_{4h} symmetry; however, adding the inner hydrogen atoms reduces its symmetry to D_{2h}.

We used several basis sets. All of them are generated from common contracted Gaussian-type functions (cGTFs), namely, Huzinaga's [53/4] set [23] on the heavy atoms and van Duijneveldt's [5/0] set [24] on the hydrogen atoms. Here the slashes divide the s and p symmetries. In the first class of basis sets (set A), the [53/4] cGTFs are split into a (521/31) valence double-zeta basis set and the 5s pGTFs are contracted to a single-zeta function. In the second class of basis sets (set B), the 5s pGTFs on hydrogen are contracted to a (41/0) double-zeta basis set. For the heavy atoms, the same valence double-zeta basis set as in set A is used, however, augmented by single s and p Rydberg functions ($\alpha = 0.008942$, 0.010430). We name this smallest basis set in class B set B_{00}. Onto this set B_{00}, we added a d polarization function ($\alpha = 0.864$ for N, 0.6 for C), a single d Rydberg function ($\alpha = 0.014782$), or both, respectively. The resulting basis sets with a d-Rydberg, a d-pol, or both a d-pol and a d-Rydberg function, respectively, added, we name set B_{01}, set B_{10}, and set B_{11}. The exponents of the d polarization functions were taken from Huzinaga et al. [23]. The exponents of the Rydberg functions were determined so that their mean *r* values equal those of the hydrogen 3*s*, 3*p*, and 3*d* atomic orbitals. The total number of cGTFs of set B_{01} and of set B_{10} is 460 and that of set B_{11} is 580. The present Rydberg functions are not enough to reproduce multiple states of a perturbed Rydberg series expressed by Eq. (1); however, we believe that the present basis sets are sufficient to examine our hypothesis discussed in the Introduction.

In CIS calculations, the restricted Hartree–Fock (RHF) molecular orbitals (MOs) obtained for the closed-shell ^1A_g ground state of the neutral molecule or for the cation ^2A_u state with an electron removed from the $2a_u$ MO are employed. In order to minimize the effects caused by the linear dependency of the basis sets, we cut some of them by projecting out the eigenvectors of the overlap matrix smaller than 10^{-4}. MOs which contain contributions of the 1s functions of the heavy atoms are kept frozen. The CSFs of $^1B_{3u}$ or $^1B_{2u}$ symmetry are generated by one-electron excitation from the closed-shell ^1A_g reference configuration. In this Tamm–Dankov CIS, the CI model space is generated in the same way as designed by Foresman et al. [7] for calculating the excited states of FBP. In order to confirm the results of the CIS calculations, sa-CASSCF calculations were also performed. The programs we employed are Gaussian 98 [25] (CIS), JAMOL4 [26] (RHF), JASON2 [27] (integral transformation), OpenMol [28] (CIS), and MOLCAS [29] (sa-CASSCF). The OpenMol CI program is based on the symmetric

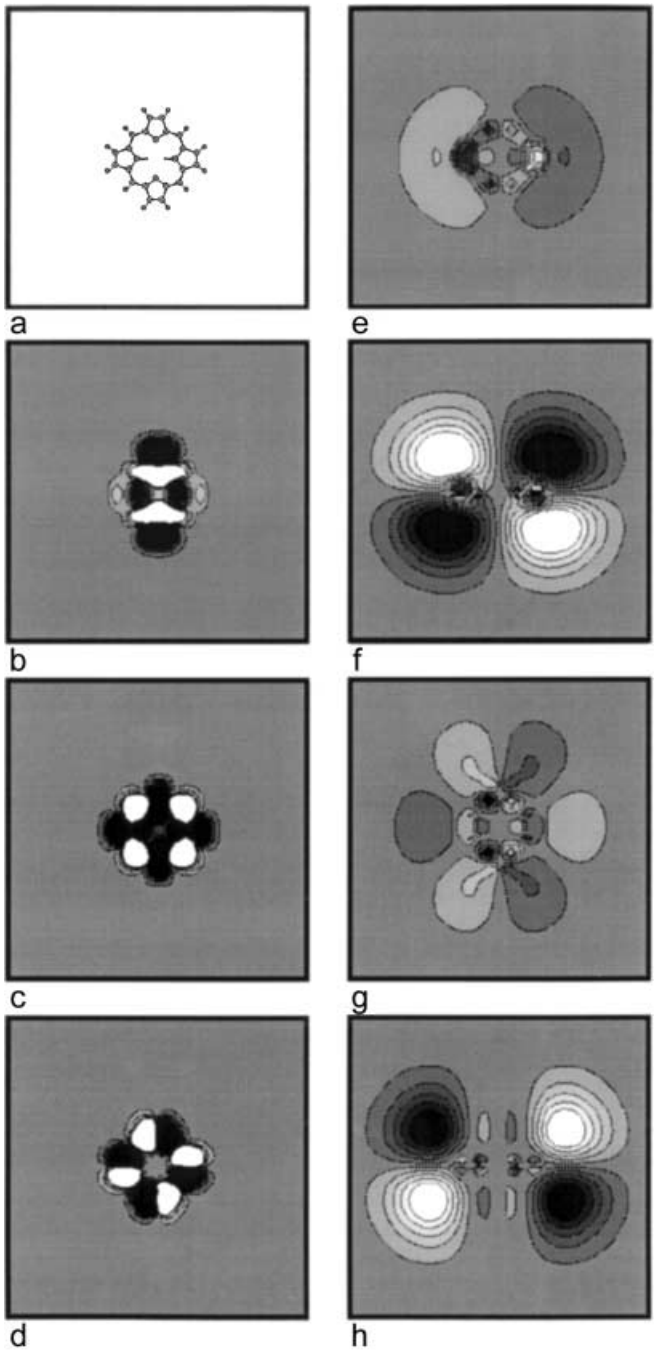

Fig. 1a–h. The restricted Hartree–Fock molecular orbitals (*MOs*) of the cation ^2A_u state. The plot region is from (−30, −30) to (+30, +30) au. **a** Molecular geometry of free-base porphin on the *xy*-plane. **b** $4b_{1u}$ MO in the plane at $z = 1$ au. **c** $5b_{1u}$ MO in the plane at $z = 1$ au. **d** $2a_u$ MO in the plane at $z = 1$ au. **e** Rydberg $5b_{2g}$ MO in the plane at $z = 1$ au. **f** Rydberg $5b_{2g}$ MO in the *yz*-plane. **g** Rydberg $6b_{2g}$ MO in the plane at $z = 1$ au. **h** Rydberg $6b_{2g}$ MO in the *yz*-plane

group graphical approach [30]. All the calculations were performed using the IBM RS/6000 SP SMP nodes at Nagoya City University.

3 Results and discussion

3.1 CIS with ^1A_g RHF MOs

First, we performed CIS calculations with the ^1A_g closed-shell ground-state RHF MOs of various basis sets. The calculated excitation energies, oscillator strengths, and dominant configurations are summarized in Table 2. The characters of the important RHF MOs obtained with set B_{10} are listed in Table 3. The $5b_{1u}$, $2a_u$, $4b_{2g}$, and $4b_{3g}$ MOs are constituents of Gouterman's four-orbital model, which he used to explain the character of the Q and B bands. Later, Yamamoto et al. [6] showed that the $4b_{1u}$ MO is also important for describing the B bands and therefore the authors included this $4b_{1u}$ MO in their five-orbital model. Above these MOs lie many p_z Rydberg orbitals of low positive orbital energy.

The leftmost column in Table 2 shows the results obtained with set A. Since this set does not include any Rydberg basis function, this column contains valence states only. By comparing with the states in the leftmost column, one can easily find the corresponding valence states obtained with different basis sets listed in the other columns. The 1-$^1B_{3u}$, 1-$^1B_{2u}$, 2-$^1B_{3u}$, and 2-$^1B_{2u}$ states are identified as Q_x, Q_y, B_x, and B_y states, respectively.

If the excited states around 4 eV above the ground state are valence states as argued by theoretical studies so far, the 3-$^1B_{3u}$ and 3-$^1B_{2u}$ states in the leftmost column of Table 2 may be assigned to the N_x and N_y bands; however, the calculated oscillator strength (2.3159) for the transition to the 3-$^1B_{3u}$ state is too large compared to the experimental value (less than 0.1) of the N bands. Table 2 also shows that by adding Rydberg functions to the basis sets Rydberg states (marked with solid circles) intrude into these valence states; therefore, the assignment of the N bands based on set A is questionable.

The columns marked set B_{00} and set B_{01} in Table 2 show that by adding d Rydberg functions to the basis sets the results of the CI calculations are not changed significantly; however, by adding d polarization functions to the basis sets, the excitation energy of the 3-$^1B_{2u}$ state drops (5.3747 eV using set B_{00} to 5.0744 eV using set B_{10}, 5.3891 eV using set B_{01} to 5.1007 eV using set B_{11}). The 4-$^1B_{3u}$ state using set B_{00}/B_{01} also drops (5.4195 eV using set B_{00} to 5.1210 eV using set B_{10}, 5.4289 eV using set B_{01} to 5.1422 eV using set B_{11}). Both states are located beneath the valence state (4-$^1B_{3u}$ using set B_{10}/B_{11}).

By adding d polarization functions to the basis set, the oscillator strength of the 3-$^1B_{2u}$ state increases from 0.0122 (set B_{00}) to 0.0337 (set B_{10}) and from 0.0085 (set B_{01}) to 0.0195 (set B_{11}). This change favorably supports the assignment of the 3-$^1B_{2u}$ state using set B_{10}/B_{11} to the N_y bands, which will be further confirmed by CIS with ^2A_u RHF MOs and sa-CASSCF calculations reported in subsequent sections. The dominant configurations of the 3-$^1B_{2u}$ state using set B_{10} are excitations from the $2a_u$ highest occupied MO to the $5b_{2g}$, $6b_{2g}$, and $7b_{2g}$ MOs. The latter MOs are diffuse p_z orbitals of Rydberg type. The use of d polarization functions stabilizes the 3-$^1B_{2u}$ and 3-$^1B_{3u}$ states as described in the preceding paragraph and increases the oscillator strength of the 3-$^1B_{2u}$ Rydberg state. It is thus shown that the d polarization function is indispensable to describe the N bands.

From the data listed in Table 2, the 2-$^1B_{2u}$ state using set B_{10}/B_{11} looks like a pure valence state ($4b_{1u}\rightarrow4b_{3g}$, $5b_{1u}\rightarrow4b_{3g}$, $2a_u\rightarrow4b_{2g}$) and there seems to be no contribution of Rydberg-type excitations. The valence-type excitations ($4b_{1u}\rightarrow4b_{2g}$, $5b_{1u}\rightarrow4b_{2g}$, $2a_u\rightarrow4b_{3g}$) are also dominant in the 2-$^1B_{3u}$ state; however, in this case the Rydberg-type excitation ($3b_{3g}\rightarrow7a_u/9a_u$) has some contribution. The 2-$^1B_{3u}$ state corresponds to the B_x band, but with some Rydberg character.

3.2 CIS with ^2A_u RHF MOs

As is well known, the RHF MOs obtained for the cation provide a better MO basis for constructing wave functions of Rydberg states than those obtained for the corresponding neutral system. For this reason, we performed CIS calculations with RHF MOs obtained for the cation ^2A_u state where one electron was removed from the $2a_u$ MO. We removed an electron from the $2a_u$ MO because the main configurations in the 3-$^1B_{2u}$ and 3-$^1B_{3u}$ states using set B_{10}/B_{11} are excitations from the $2a_u$ MO as shown in Table 2. Since the effect of d polarization functions is demonstrated clearly in set B_{10} and the size of set B_{10} is feasible, we used only this set here. To handle the open-shell cation system, we used the JAMOL4 [26] and OpenMol [28] programs.

The computational results are summarized in Table 4. The CIS eigenvectors are listed in the order of calculated excitation energies with the correlation correction which will be discussed soon. The total number of CSFs for the ^1A_g, $^1B_{3u}$, and $^1B_{2u}$ states are 2935, 2922, and 2914, respectively. The contour maps of the Rydberg-type MOs ($5b_{2g}$, $6b_{2g}$, $5b_{3g}$, $6b_{3g}$) are displayed in Fig. 1. They have much weight on the C_β and C_m atoms as well as on the nitrogen atoms.

As seen from Table 4, the dominant configuration of the 2-$^1B_{2u}$ CIS state results from the ($2a_u\rightarrow5b_{2g}$) excitation when the ^2A_u RHF MOs are used. As shown in Fig. 1f, the $5b_{2g}$ MO has the spatial extension of a typical Rydberg orbital; therefore, the 2-$^1B_{2u}$ state is a pure Rydberg state. This state corresponds to the 3-$^1B_{2u}$ state using set B_{10} displayed in Table 2. The 3-$^1B_{2u}$ state in Table 4 is predominantly a valence state ($5b_{1u}\rightarrow4b_{3g}$, $2a_u\rightarrow4b_{2g}$) with a Rydberg-type contribution ($2a_u\rightarrow6b_{2g}$). The CIS 3-$^1B_{2u}$ state in Table 4 corresponds to the 2-$^1B_{2u}$ state using set B_{10} in Table 2.

In the case of the $^1B_{3u}$ symmetry, both 2-$^1B_{3u}$ and 3-$^1B_{3u}$ states exhibit the mixing of Rydberg and valence characters, i.e., larger Rydberg and smaller valence characters for 2-$^1B_{3u}$ and larger valence and smaller Rydberg characters for 3-$^1B_{3u}$. As in the case of $^1B_{2u}$, the use of the ^2A_u RHF MOs reverses the order of 2-$^1B_{3u}$ and 3-$^1B_{3u}$ in Table 3. Thus, the use of MOs obtained

Table 2. CI singles (CIS) wave functions obtained by using Gaussian 98 and ^1A_g restricted Hartree–Fock (*RHF*) molecular orbitals (*MOs*). The ^1A_g RHF energy is –982.9652 au. *Solid circles* denote Rydberg states. *Diamond symbols* show that the oscillator strength (*f*) is increased by adding d polarization functions. *Asterisks* denote that the listings of the entries are shifted beyond the 3-$^1B_{3u}$ state to make the table compact. CI coefficients whose magnitude is greater than 0.1 are listed. No Rydberg functions are included in set A

Set A	Set B_{00}	Set-B_{01}	Set B_{10}	Set B_{11}
1-$^1B_{3u}$	1-$^1B_{3u}$	1-$^1B_{3u}$	1-$^1B_{3u}$	1-$^1B_{3u}$
2.4588 eV	2.4761 eV	2.4778 eV	2.4068 eV	2.4082 eV
f = 0.0020	f = 0.0012	f = 0.0013	f = 0.0222	f = 0.0229
$5b_{1u}\rightarrow4b_{2g}$ = 0.495	$5b_{1u}\rightarrow4b_{2g}$ = 0.496	$5b_{1u}\rightarrow4b_{2g}$ = −0.494	$5b_{1u}\rightarrow4b_{2g}$ = 0.463	$5b_{1u}\rightarrow4b_{2g}$ = −0.462
$2a_u\rightarrow4b_{3g}$ = −0.483	$2a_u\rightarrow4b_{3g}$ = 0.482	$2a_u\rightarrow4b_{3g}$ = −0.484	$2a_u\rightarrow4b_{3g}$ = 0.513	$2a_u\rightarrow4b_{3g}$ = −0.514
1-$^1B_{2u}$	1-$^1B_{2u}$	1-$^1B_{2u}$	1-$^1B_{2u}$	1-$^1B_{2u}$
2.5977 eV	2.6051 eV	2.6029 eV	2.5010 eV	2.4992 eV
f = 0.0281	f = 0.0234	f = 0.0240	f = 0.0456	f = 0.0466
$5b_{1u}\rightarrow4b_{3g}$ = 0.447	$5b_{1u}\rightarrow4b_{3g}$ = −0.450	$5b_{1u}\rightarrow4b_{3g}$ = 0.449	$5b_{1u}\rightarrow4b_{3g}$ = −0.432	$5b_{1u}\rightarrow4b_{3g}$ = 0.431
$2a_u\rightarrow4b_{2g}$ = 0.529	$2a_u\rightarrow4b_{2g}$ = 0.526	$2a_u\rightarrow4b_{2g}$ = −0.527	$2a_u\rightarrow4b_{2g}$ = 0.539	$2a_u\rightarrow4b_{2g}$ = −0.541
2-$^1B_{3u}$	2-$^1B_{3u}$	2-$^1B_{3u}$	2-$^1B_{3u}$	2-$^1B_{3u}$
4.4099 eV	4.4467 eV	4.4411 eV	4.3997 eV	4.3955 eV
f = 1.2060	f = 1.3221	f = 1.3726	f = 1.2713	f = 1.3224
$4b_{1u}\rightarrow4b_{2g}$ = 0.414	$4b_{1u}\rightarrow4b_{2g}$ = −0.404	$4b_{1u}\rightarrow4b_{2g}$ = −0.398	$4b_{1u}\rightarrow4b_{2g}$ = 0.405	$4b_{1u}\rightarrow4b_{2g}$ = −0.399
$3b_{3g}\rightarrow3a_u$ = 0.158	$3b_{3g}\rightarrow7a_u$ = 0.153	$3b_{3g}\rightarrow9a_u$ = 0.139	$3b_{3g}\rightarrow7a_u$ = −0.162	$3b_{3g}\rightarrow9a_u$ = −0.139
$5b_{1u}\rightarrow4b_{2g}$ = 0.355	$5b_{1u}\rightarrow4b_{2g}$ = −0.361	$5b_{1u}\rightarrow4b_{2g}$ = −0.367	$5b_{1u}\rightarrow4b_{2g}$ = 0.390	$5b_{1u}\rightarrow4b_{2g}$ = −0.395
$2a_u\rightarrow4b_{3g}$ = 0.397	$2a_u\rightarrow4b_{3g}$ = 0.402	$2a_u\rightarrow4b_{3g}$ = 0.403	$2a_u\rightarrow4b_{3g}$ = −0.369	$2a_u\rightarrow4b_{3g}$ = 0.370
2-$^1B_{2u}$	2-$^1B_{2u}$	2-$^1B_{2u}$	2-$^1B_{2u}$	2-$^1B_{2u}$
4.8007 eV	4.7622 eV	4.7378 eV	4.7262 eV	4.7012 eV
f = 2.9300	f = 2.9108	f = 2.9215	f = 2.7890	f = 2.8135
$4b_{1u}\rightarrow4b_{3g}$ = 0.125	$4b_{1u}\rightarrow4b_{3g}$ = 0.120	$4b_{1u}\rightarrow4b_{3g}$ = 0.119	$4b_{1u}\rightarrow4b_{3g}$ = 0.124	$4b_{1u}\rightarrow4b_{3g}$ = −0.123
$5b_{1u}\rightarrow4b_{3g}$ = 0.518	$5b_{1u}\rightarrow4b_{3g}$ = 0.512	$5b_{1u}\rightarrow4b_{3g}$ = 0.513	$5b_{1u}\rightarrow4b_{3g}$ = 0.524	$5b_{1u}\rightarrow4b_{3g}$ = −0.526
$2a_u\rightarrow4b_{2g}$ = −0.435	$2a_u\rightarrow4b_{2g}$ = 0.436	$2a_u\rightarrow4b_{2g}$ = 0.435	$2a_u\rightarrow4b_{2g}$ = 0.417	$2a_u\rightarrow4b_{2g}$ = −0.415
	3-$^1B_{2u}$ •*	3-$^1B_{2u}$ •*	3-$^1B_{2u}$ •	3-$^1B_{2u}$ •
	5.3747 eV	5.3891 eV	5.0744 eV	5.1007 eV
	f = 0.0122	f = 0.0085	f = 0.0337 ◆	f = 0.0195 ◆
	$2a_u\rightarrow5b_{2g}$ = 0.635	$2a_u\rightarrow5b_{2g}$ = 0.622	$2a_u\rightarrow5b_{2g}$ = 0.634	$2a_u\rightarrow5b_{2g}$ = −0.622
	$2a_u\rightarrow6b_{2g}$ = −0.120	$2a_u\rightarrow7b_{2g}$ = 0.233	$2a_u\rightarrow6b_{2g}$ = −0.119	$2a_u\rightarrow7b_{2g}$ = −0.232
	$2a_u\rightarrow7b_{2g}$ = −0.255	$2a_u\rightarrow8b_{2g}$ = −0.185	$2a_u\rightarrow7b_{2g}$ = −0.254	$2a_u\rightarrow8b_{2g}$ = 0.185
	4-$^1B_{3u}$ •*	4-$^1B_{3u}$ •*	3-$^1B_{3u}$ •	3-$^1B_{3u}$ •
	5.4195 eV	5.4289 eV	5.1210 eV	5.1422 eV
	f = 0.0059	f = 0.0029	f = 0.0028	f = 0.0088
	$2a_u\rightarrow5b_{3g}$ = 0.636	$2a_u\rightarrow5b_{3g}$ = −0.622	$2a_u\rightarrow5b_{3g}$ = 0.637	$2a_u\rightarrow5b_{3g}$ = 0.622
	$2a_u\rightarrow7b_{3g}$ = −0.258	$2a_u\rightarrow7b_{3g}$ = 0.233	$2a_u\rightarrow7b_{3g}$ = −0.258	$2a_u\rightarrow7b_{3g}$ = −0.233
		$2a_u\rightarrow8b_{3g}$ = 0.118		$2a_u\rightarrow8b_{3g}$ = −0.116
		$2a_u\rightarrow9b_{3g}$ = −0.147		$2a_u\rightarrow9b_{3g}$ = 0.148
3-$^1B_{3u}$	3-$^1B_{3u}$	3-$^1B_{3u}$	4-$^1B_{3u}$	4-$^1B_{3u}$
5.2549 eV	5.2476 eV	5.2293 eV	5.2211 eV	5.2002 eV
f = 2.3159	f = 2.2213	f = 2.1700	f = 2.2030	f = 2.1441
$4b_{1u}\rightarrow4b_{2g}$ = 0.513	$4b_{1u}\rightarrow4b_{2g}$ = 0.520	$4b_{1u}\rightarrow4b_{2g}$ = −0.525	$4b_{1u}\rightarrow4b_{2g}$ = 0.514	$4b_{1u}\rightarrow4b_{2g}$ = −0.518
$3b_{3g}\rightarrow3a_u$ = 0.148	$3b_{3g}\rightarrow7a_u$ = −0.152	$3b_{3g}\rightarrow9a_u$ = 0.140	$3b_{3g}\rightarrow7a_u$ = −0.153	$3b_{3g}\rightarrow9a_u$ = −0.131
$5b_{1u}\rightarrow4b_{2g}$ = −0.327	$5b_{1u}\rightarrow4b_{2g}$ = −0.317	$5b_{1u}\rightarrow4b_{2g}$ = 0.315	$5b_{1u}\rightarrow4b_{2g}$ = −0.330	$5b_{1u}\rightarrow4b_{2g}$ = 0.324
$2a_u\rightarrow4b_{3g}$ = −0.290	$2a_u\rightarrow4b_{3g}$ = 0.281	$2a_u\rightarrow4b_{3g}$ = −0.276	$2a_u\rightarrow4b_{3g}$ = 0.274	$2a_u\rightarrow4b_{3g}$ = −0.268
	5-$^1B_{3u}$ •	5-$^1B_{3u}$ •	5-$^1B_{3u}$ •	5-$^1B_{3u}$ •
	5.5568 eV	5.5753 eV	5.5929 eV	5.6216 eV
	f = 0.0073	f = 0.0046	f = 0.0073	f = 0.0050
	$5b_{1u}\rightarrow5b_{2g}$ = 0.628	$5b_{1u}\rightarrow5b_{2g}$ = 0.615	$5b_{1u}\rightarrow5b_{2g}$ = 0.627	$5b_{1u}\rightarrow5b_{2g}$ = −0.612
	$5b_{1u}\rightarrow6b_{2g}$ = −0.122	$5b_{1u}\rightarrow7b_{2g}$ = 0.239	$5b_{1u}\rightarrow6b_{2g}$ = −0.124	$5b_{1u}\rightarrow7b_{2g}$ = −0.240
	$5b_{1u}\rightarrow7b_{2g}$ = −0.263	$5b_{1u}\rightarrow8b_{2g}$ = −0.192	$5b_{1u}\rightarrow7b_{2g}$ = −0.265	$5b_{1u}\rightarrow8b_{2g}$ = 0.196
				$5b_{1u}\rightarrow13b_{2g}$ = −0.101
	4-$^1B_{2u}$ •	4-$^1B_{2u}$ •	4-$^1B_{2u}$ •	
	5.6266 eV	5.6371 eV	5.6650 eV	
	f = 0.0006	f = 0.0006	f = 0.0019	
	$5b_{1u}\rightarrow5b_{3g}$ = 0.632	$5b_{1u}\rightarrow5b_{3g}$ = −0.620	$5b_{1u}\rightarrow5b_{3g}$ = 0.629	
	$5b_{1u}\rightarrow6b_{3g}$ = 0.109	$5b_{1u}\rightarrow7b_{3g}$ = 0.242	$5b_{1u}\rightarrow6b_{3g}$ = 0.107	
	$5b_{1u}\rightarrow7b_{3g}$ = −0.262	$5b_{1u}\rightarrow8b_{3g}$ = 0.123	$5b_{1u}\rightarrow7b_{3g}$ = −0.264	
	$5b_{1u}\rightarrow9b_{3g}$ = 0.108	$5b_{1u}\rightarrow9b_{3g}$ = −0.142	$5b_{1u}\rightarrow9b_{3g}$ = 0.108	
3-$^1B_{2u}$	5-$^1B_{2u}$	5-$^1B_{2u}$		
5.9897 eV	5.9776 eV	5.9628 eV		
f = 0.4516	f = 0.3950	f = 0.3957		
$3b_{1u}\rightarrow4b_{3g}$ = 0.173	$3b_{1u}\rightarrow4b_{3g}$ = 0.194	$3b_{1u}\rightarrow4b_{3g}$ = 0.193		
$4b_{1u}\rightarrow4b_{3g}$ = 0.653	$4b_{1u}\rightarrow4b_{3g}$ = −0.640	$4b_{1u}\rightarrow4b_{3g}$ = −0.642		

for the cation ^2A_u state exchanges the order of the valencelike state and the Rydberg-like state.

For the fourth states, mixing of the valence- and Rydberg-type excitations is observed and the Rydberg-type excitations dominate for the fifth $^1B_{3u}$ and $^1B_{2u}$ states.

The ($4b_{1u}\rightarrow 4b_{2g}$) excitation appears in the 2-$^1B_{3u}$, 3-$^1B_{3u}$, and 4-$^1B_{3u}$ states. Similarly, the ($5b_{1u}\rightarrow 4b_{3g}$) excitation appears in the 3-$^1B_{2u}$ and 4-$^1B_{2u}$ states. Their CI coefficients suggest that these configurations are series perturbers (Table 4).

Table 3. ^1A_g RHF MOs obtained by using Gaussian 98 and set B_{10}. MOs which appear in the CIS dominant configurations are listed

Seq.[a]	Symmetry	MO energy	Character
143	$7a_u$	0.11345	p_z Rydberg
137	$9b_{3g}$	0.09179	p_z Rydberg
136	$9b_{2g}$	0.09115	p_z Rydberg
117	$7b_{3g}$	0.06064	p_z Rydberg
114	$7b_{2g}$	0.05929	p_z Rydberg
103	$6b_{2g}$	0.04166	p_z Rydberg
102	$6b_{3g}$	0.04136	p_z Rydberg
93	$5b_{3g}$	0.02907	p_z Rydberg
92	$5b_{2g}$	0.02738	p_z Rydberg
83	$4b_{3g}$	0.00919	π^*, nLUMO
82	$4b_{2g}$	0.00548	π^*, LUMO
81	$2a_u$	−0.22619	π, HOMO
80	$5b_{1u}$	−0.24641	π, nHOMO
79	$3b_{3g}$	−0.33140	π, HOMO-2
78	$4b_{1u}$	−0.33833	π, HOMO-3
77	$3b_{2g}$	−0.37125	π
76	$2b_{3g}$	−0.38197	π
75	$2b_{2g}$	−0.38615	π
74	$3b_{1u}$	−0.38755	π

[a] Sequential number in order of orbital energy

3.3 Correlation correction to CIS

Since electron correlation effects are not accounted for by the CIS method, the computed excitation energy is much higher than the experimental value. To evaluate the correlation energy, we need to perform a more sophisticated calculation such as MRCISD; however, such a calculation requires quite a high computational cost for the extended basis sets employed here. Instead, we here correct the CIS excitation energy of the perturbed states (excepting the 1-$^1B_{3u}$ and 1-$^1B_{2u}$ states) by using the following empirical formula.

$$\mathrm{EE_{estim}} = \mathrm{EE_{CIS}} - \Delta E_{\mathrm{val}}\left(\sum_{\mathrm{v}} C_{\mathrm{v}}^2\right) - \Delta E_{\mathrm{R}}\left(\sum_{\mathrm{R}} C_{\mathrm{R}}^2\right) , \quad (3)$$

where $\mathrm{EE_{estim}}$ is the estimated excitation energy in electron volts, $\mathrm{EE_{CIS}}$ is the excitation energy calculated by the CIS method, ΔE_{val} is the decrease of the valence-type excitation energy by correlation effects and orbital reorganization, C_{v} is the CI coefficient of the valence-type excitation, ΔE_{R} is the decrease of the Rydberg-type excitation energy by correlation effects and orbital reorganization, and C_{R} is the CI coefficient of the Rydberg-type excitation.

We have assumed ΔE_{val} and ΔE_{R} to be constant for all the states except for the lowest $^1B_{3u}$ and $^1B_{2u}$ states.

Table 4. CIS wave functions obtained by using OpenMol and ^2A_u RHF MOs. The ^2A_u RHF energy is −982.7540 au. The ^1A_g CIS energy is −982.9671. The CI dimensions for the ^1A_g, $^1B_{3u}$, and $^1B_{2u}$ states are 2,935, 2,922, and 2,914, respectively. The *solid circles* denote Rydberg-type MOs. The symbols *v* and *R* denote valence- and Rydberg-type excitations, respectively. *EE* denotes the excitation energy (eV). CI coefficients whose magnitude is greater than 0.1 are listed

Symmetry	EE (eV)	Configuration	CI coefficient	Excitation type	$\mathrm{EE_{estim}}$[a]	Assignment[b]
1-$^1B_{3u}$	2.8640	$2a_u\rightarrow 4b_{3g}$	0.754525	v	2.86	Q_x (1.98)
		$5b_{1u}\rightarrow 4b_{2g}$	0.623546	v		
		$2b_{3g}\rightarrow 3a_u$	−0.112319	v		
1-$^1B_{2u}$	2.9489	$2a_u\rightarrow 4b_{2g}$	0.785364	v	2.95	Q_y (2.42)
		$5b_{1u}\rightarrow 4b_{3g}$	−0.584574	v		
		$3b_{2g}\rightarrow 3a_u$	0.128416	v		
3-$^1B_{3u}$	4.8161	$2a_u\rightarrow 5b_{3g}$ •	0.529344	R	3.08	B_x (3.33)
		$5b_{1u}\rightarrow 4b_{2g}$	−0.498800	v		
		$4b_{1u}\rightarrow 4b_{2g}$	0.450429	v		
		$2a_u\rightarrow 4b3_g$	0.439675	v		
		$3b_{3g}\rightarrow 3a_u$	0.185274	v		
3-$^1B_{2u}$	5.1530	$5b_{1u}\rightarrow 4b_{3g}$	−0.744197	v	3.33	B_y (3.33)
		$2a_u\rightarrow 4b_{2g}$	−0.546733	v		
		$2a_u\rightarrow 6b_{2g}$ •	−0.177012	R		
2-$^1B_{3u}$	4.8005	$2a_u\rightarrow 5b_{3g}$ •	0.844668	R	3.44	N_x (3.65)
		$5b_{1u}\rightarrow 4b_{2g}$	0.313927	v		
		$4b_{1u}\rightarrow 4b_{2g}$	−0.283045	v		
		$2a_u\rightarrow 4b_{3g}$	−0.272300	v		
		$3b_{3g}\rightarrow 3a_u$	−0.114024	v		
2-$^1B_{2u}$	4.7543	$2a_u\rightarrow 5b_{2g}$ •	0.993377	R	3.65	N_y (3.65)
4-$^1B_{3u}$	5.4784	$2a_u\rightarrow 6b_{3g}$ •	0.983053	R	4.35	L_x (4.67)
		$4b_{1u}\rightarrow 4b_{2g}$	0.146908	v		
4-$^1B_{2u}$	5.5023	$2a_u\rightarrow 6b_{2g}$ •	−0.981811	R	4.39	L_y (4.67)
		$5b_{1u}\rightarrow 4b_{3g}$	0.132377	v		
5-$^1B_{2u}$	5.6465	$2a_u\rightarrow 7b_{2g}$ •	0.996775	R	4.53	M_y (5.50)
5-$^1B_{3u}$	5.6889	$2a_u\rightarrow 7b_{3g}$ •	−0.989360	R	4.59	M_x (5.50)

[a] Excitation energy corrected by the estimated electron correlation energy
[b] Experimental excitation energy is given in parentheses

We first determine ΔE_R. From Tables 2 and 4, we consider that the pure Rydberg-type configuration ($2a_u \rightarrow 5b_{2g}$) is a good candidate for the N_y state, and we estimate ΔE_R by substituting the experimental excitation energy (3.65 eV) of the N_y bands for EE_{estim} in Eq. (3): $\Delta E_R = (EE_{CIS} - EE_{estim}) \Big/ \left(\sum_R C_R^2 \right)$. Then ΔE_R is calculated to be 1.12 eV. Secondly we consider ΔE_{val}. Tables 1 and 2 illustrate that the correlation effects decrease the excitation energies of the valencelike states. By applying Eq. (3) to the B_y bands and using its experimental excitation energy (3.3 eV), EE_{CIS} (5.1530 eV), and ΔE_R (1.12 eV), we estimated ΔE_{val} as 2.10 eV. Here, have counted the CI coefficients whose magnitude is greater than 0.1.

The estimated excitation energies are given in the second column from the right in Table 4. We analyze the results from the aspects of excitation energetics and the characteristics of the excited states. Table 4 shows that the calculated excitation energies are in good agreement with experiments. Thus, we assign the 3-$^1B_{2u}$ and 2-$^1B_{2u}$ states listed in Table 4 to the B_y and N_y bands and 3-$^1B_{3u}$ and 2-$^1B_{3u}$ to B_x and N_x, respectively. Next, we verify this assignment not only by using the CI coefficients in Table 4 but also by using the oscillator strengths in Table 2. The reason we also use Table 2 here is that the current version of the OpenMol program which was used to perform CIS/^2A_u MOs cannot evaluate oscillator strength between two states of different symmetry. In the B_x and N_x states, the CI coefficients of the ($2a_u \rightarrow 4b_{3g}$) and ($5b_{1u} \rightarrow 4b_{2g}$) excitations have almost equal magnitude with opposite sign. This pair of configurations will increase the oscillator strength [17, 31]. We expect that the B_x and N_x bands will have considerable oscillator strengths but with f_{Bx} much larger than f_{Nx}, which is in accord with the experimental oscillator strength. The calculated oscillator strength (0.0028) for the N_x bands by CIS with set B_{10} is also consistent with the experiment (below 0.1). Concerning the N_y state, both CIS/^2A_u MOs and CIS/^1A_g MOs predict that this state is almost pure Rydberg-type and its oscillator strength is 0.0337, being consistent with the experiments. All the considerations show that our assignment for the excited states is appropriate.

Usually the correlated ionization potential (IP) is larger than the SCF IP because the correlation energy for the ground state is larger than that for the ionized state. From this reason, one may question why the correction in Eq. (3) decreases the excitation energies of Rydberg-like states ($-\Delta E_R$). We consider that this arises from the limitation of the CIS/^2A_u MOs calculation; namely, incomplete orbital reorganization especially for the low-lying Rydberg states. In order to confirm this conjecture, we show the results of sa-CASSCF calculations in the next section.

3.4 State-averaged CASSCF

In order to eliminate the unclearness in the preceding CIS/^2A_u calculation induced from the orbital reorganization, we performed sa-CASSCF calculations by using set B_{10} and the MOLCAS program [29]. We chose 12 MOs (4–$5b_{1u}$, 4–$7b_{2g}$, $2a_u$, 3–$7b_{3g}$) as the active orbitals and averaged the low-lying six states. Individual sa-CASSCF calculations were performed for the $^1B_{3u}$ and $^1B_{2u}$ symmetries. Distributing eight electrons among these 12 MOs generates a complete active space of 17496 CSFs. The excitation energies, important configurations, their coefficients, and their weights of the sa-CASSCF calculations are given in Table 5. For simplicity, the ^1A_g RHF total energy is used as the base value to calculate the excitation energies. The results given by CIS and sa-CASSCF are summarized in Table 6 and the final assignments are shown.

The N_y state, which was calculated to be a pure Rydberg state by the CIS calculations, is the 3−1 B_{2u} in sa-CASSCF. Its excitation energy is 4.07 eV and the wave function is mostly composed of Rydberg-type CSFs with a small portion of the valence-type CSFs (Table 5), being consistent with the preceding CIS calculations. The consistency of the results verifies the validity of the negative correlation correction ($-\Delta E_R = -1.12$ eV) for Rydberg-type excitations in Eq. (3).

Let us discuss the entire spectra in detail. All the excitation energies given by sa-CASSCF agree well with the experiments except for the valencelike states found at 4.68 and 4.98 eV, which will be discussed later. Table 6 also shows that the estimated excitation energies given by CIS/^2A_u MOs are appropriate. Regarding the character of the excited states, the correspondence between the CIS/^1A_g MOs and sa-CASSCF calculations is reasonable at the qualitative level. We assign the first $^1B_{3u}$ and $^1B_{2u}$ states to the Q bands and the second $^1B_{3u}$ and $^1B_{2u}$ states to the B bands. It seems pertinent to assign the third $^1B_{3u}$ and $^1B_{2u}$ states to the N bands. Both states are pure Rydberg states or the perturbed Rydberg states and their oscillator strengths calculated by CIS/^1A_g MOs are quite consistent with the experimental values. Finally, we comment that the state assigned to 4.25L by the experiments does not appear in the CIS/^2A_u MOs calculation. This is because this state arises from excitations not from the $2a_u$ but from the $5b_{1u}$ MO.

As is well known, the CASSCF method evaluates mainly nondynamical electron correlation effects. If the remaining dynamical correlation effects were fully taken into account, the role of the valence states at 4.68 and 4.98 eV would be clarified. These states would mix with the N_x state (at 4.13 eV by sa-CASSCF) or the N_y state (at 4.07 eV) to some extent, giving lower excitation energies. They may also affect the higher Rydberg states, giving larger oscillator strengths. Determining their accurate characteristics is the main subject of our next research project.

4 Concluding remarks

Guided by the small oscillator strengths of the N bands and by the comparatively large oscillator strengths of the higher states, we have applied the model of a perturbed Rydberg series for the FBP excited states. By using extended basis sets including s, p, and d Rydberg functions and d polarization functions, we have found

Table 5. State-averaged complete-active-space self-consistent-field wave functions obtained by using MOLCAS. The configurations whose weight is greater than 0.01 are listed. The symbols *v* and *R* denote valence- and Rydberg-type excitations, respectively

Symmetry	EE (eV)[a]	Total energy	$\langle z^2 \rangle$[b]	Configuration	Coefficient	Weight	Excitation type
1-$^1B_{3u}$	2.07	−982.889092	−112.05				
				$5b_{1u} \rightarrow 4b_{2g}$	0.74573	0.55611	v
				$2a_u \rightarrow 4b_{3g}$	−0.59434	0.35324	v
				$4b_{1u} \rightarrow 4b_{2g}$	0.13331	0.01777	v
				$5b_{1u}, 3b_{3g} \rightarrow 4b_{2g}, 4b_{3g}$	−0.12402	0.01538	v
				$2a_u, 3b_{3g} \rightarrow 4b_{2g}, 4b_{2g}$	−0.10469	0.01096	v
				$5b_{1u}, 5b_{1u}, 2a_u \rightarrow 4b_{2g}, 4b_{2g}, 4b_{3g}$	−0.10399	0.01081	v
1-$^1B_{2u}$	2.38	−982.877717	−112.08				
				$2a_u \rightarrow 4b_{2g}$	0.71003	0.50414	v
				$5b_{1u} \rightarrow 4b_{3g}$	−0.66164	0.43777	v
2-$^1B_{3u}$	3.41	−982.839590	−112.10				
				$2a_u \rightarrow 4b_{3g}$	−0.66459	0.44169	v
				$4b_{1u} \rightarrow 4b_{2g}$	−0.51731	0.26761	v
				$5b_{1u} \rightarrow 4b_{2g}$	−0.39030	0.15233	v
				$5b_{1u}, 2a_u, 2a_u \rightarrow 4b_{2g}, 4b_{3g}, 4b_{3g}$	0.19473	0.03792	v
				$2a_u, 3b_{3g} \rightarrow 4b_{2g}, 4b_{2g}$	0.16775	0.02814	v
				$5b_{1u}, 3b_{3g} \rightarrow 4b_{2g}, 4b_{3g}$	0.14606	0.02133	v
2-$^1B_{2u}$	3.95	−982.819755	−117.80				
				$5b_{1u} \rightarrow 4b_{3g}$	0.59732	0.35679	v
				$2a_u \rightarrow 4b_{2g}$	0.58576	0.34311	v
				$4b_{1u} \rightarrow 4b_{3g}$	0.30110	0.09066	v
				$5b_{1u}, 2a_u, 2a_u \rightarrow 4b_{2g}, 4b_{2g}, 4b_{3g}$	−0.19497	0.03801	v
				$2a_u \rightarrow 6b_{2g}$	0.18211	0.03316	R
				$2a_u \rightarrow 5b_{2g}$	0.16539	0.02736	R
				$5b_{1u}, 5b_{1u}, 2a_u \rightarrow 4b_{2g}, 4b_{3g}, 4b_{3g}$	−0.15749	0.02480	v
				$5b_{1u}, 3b_{3g} \rightarrow 4b_{3g}, 4b_{3g}$	0.15359	0.02359	v
				$5b_{1u} \rightarrow 5b_{3g}$	0.11704	0.01370	R
3-$^1B_{2u}$	4.07	−982.815650	−178.70				
				$2a_u \rightarrow 5b_{2g}$	0.75624	0.57190	R
				$2a_u \rightarrow 6b_{2g}$	0.55093	0.30352	R
				$2a_u \rightarrow 4b_{2g}$	−0.15333	0.02351	v
				$5b_{1u} \rightarrow 4b_{3g}$	−0.14811	0.02194	v
				$5b_{1u}, 2a_u, 2a_u \rightarrow 4b_{2g}, 5b_{2g}, 4b_{3g}$	−0.10763	0.01158	R
3-$^1B_{3u}$	4.13	−982.813418	−182.66				
				$2a_u \rightarrow 5b_{3g}$	−0.95488	0.91179	R
				$2a_u \rightarrow 6b3_g$	−0.15576	0.02426	R
				$5b_{1u}, 2a_u, 2a_u \rightarrow 4b_{2g}, 4b_{3g}, 5b_{3g}$	0.13335	0.01778	R
4-$^1B_{3u}$	4.31	−982.806645	−182.85				
				$5b_{1u} \rightarrow 5b_{2g}$	0.94695	0.89671	R
				$5b_{1u}, 3b_{3g} \rightarrow 5b_{2g}, 4b_{3g}$	−0.12810	0.01641	R
				$5b_{1u}, 2a_u, 2a_u \rightarrow 4b_{2g}, 4b_{2g}, 5b_{2g}$	0.12674	0.01606	R
				$5b_{1u}, 5b_{1u}, 2a_u \rightarrow 4b_{2g}, 5b_{2g}, 4b_{3g}$	−0.11402	0.01300	R
4-$^1B_{2u}$	4.36	−982.804860	−181.32				
				$5b_{1u} \rightarrow 5b_{3g}$	0.93787	0.87959	R
				$2a_u, 3b_{3g} \rightarrow 4b_{2g}, 5b_{3g}$	0.11250	0.01266	R
				$5b_{1u}, 3b_{3g} \rightarrow 4b_{3g}, 5b_{3g}$	0.10478	0.01098	R
				$5b_{1u}, 5b_{1u}, 2a_u \rightarrow 4b_{2g}, 4b_{3g}, 5b_{3g}$	−0.10114	0.01023	R
5-$^1B_{3u}$	4.68	−982.793178	−118.86				
				$4b_{1u} \rightarrow 4b_{2g}$	−0.71513	0.51142	v
				$5b_{1u} \rightarrow 4b_{2g}$	0.41538	0.17254	v
				$2a_u \rightarrow 4b_{3g}$	0.31354	0.09831	v
				$2a_u \rightarrow 6b_{3g}$	−0.30057	0.09034	R
				$2a_u, 3b_{3g} \rightarrow 4b_{2g}, 4b_{2g}$	0.19183	0.03680	v
				$5b_{1u}, 5b_{1u}, 2a_u \rightarrow 4b_{2g}, 4b_{2g}, 4b_{3g}$	−0.15972	0.02551	v
				$4b_{1u}, 5b_{1u}, 2a_u \rightarrow 4b_{2g}, 4b_{2g}, 4b_{3g}$	0.10530	0.01109	v
				$5b_{1u}, 2a_u, 2a_u \rightarrow 4b_{2g}, 4b_{3g}, 4b_{3g}$	−0.10457	0.01093	v
5-$^1B_{2u}$	4.74	−982.790923	−181.45				
				$2a_u \rightarrow 6b_{2g}$	0.77207	0.59609	R
				$2a_u \rightarrow 5b_{2g}$	−0.57835	0.33448	R
				$5b_{1u}, 2a_u, 2a_u \rightarrow 4b_{2g}, 6b_{2g}, 4b_{3g}$	−0.10996	0.01209	R

Table 5. (Contd.)

Symmetry	EE (eV)[a]	Total energy	$\langle z^2 \rangle$[b]	Configuration	Coefficient	Weight	Excitation type
6-$^1B_{3u}$	4.76	−982.790179	−174.54				
				$2a_u \rightarrow 6b_{3g}$	−0.90643	0.82162	R
				$4b_{1u} \rightarrow 4b_{2g}$	0.22567	0.05093	v
				$2a_u \rightarrow 5b_{3g}$	0.14429	0.02082	R
				$5b_{1u} \rightarrow 4b_{2g}$	−0.14289	0.02042	v
				$5b_{1u}$, $2a_u$, $2a_u \rightarrow 4b_{2g}$, $4b_{3g}$, $6b_{3g}$	0.12655	0.01601	R
				$2a_u \rightarrow 4b_{3g}$	−0.12441	0.01548	v
6-$^1B_{2u}$	4.98	−982.781889	−112.22				
				$4b_{1u} \rightarrow 4b_{3g}$	−0.86749	0.75254	v
				$5b_{1u} \rightarrow 4b_{3g}$	0.28071	0.07880	v
				$2a_u \rightarrow 4b_{2g}$	0.18301	0.03349	v
				$2a_u$, $3b_{3g} \rightarrow 4b_{2g}$, $4b_{3g}$	−0.17919	0.03211	v
				$5b_{1u}$, $3b_{3g} \rightarrow 4b_{3g}$, $4b_{3g}$	−0.16974	0.02881	v
				$5b_{1u}$, $5b_{1u}$, $2a_u \rightarrow 4b_{2g}$, $4b_{3g}$, $4b_{3g}$	−0.14070	0.01980	v

[a] Excitation energy based on the ^1A_g RHF energy
[b] The expectation value of electronic second moment

Table 6. Final assignment of the $^1B_{3u}$ and $^1B_{2u}$ excited states of FBP. Oscillator strengths are given in *brackets*. *R* (or *v*) denotes Rydberg (valence) configurations dominant. **R + v** (or *v* + *R*) means mixing of valance configurations into dominant Rydberg configurations (vice versa). Solid circles denote Rydberg orbitals. Experimental excitation energies are given in *parentheses*

Configuration[a]	Symmetry	CIS/^1A_g MO	CIS/^2A_u MO	sa-CASSCF	Assignment
$2a_u \rightarrow 4b_{3g}$ $5b_{1u} \rightarrow 4b_{2g}$	$^1B_{3u}$	2.41 (v) [0.0222]	2.86 (v)	2.07 (v)	Q_x (1.98) [0.01]
$2a_u \rightarrow 4b_{2g}$ $5b_{1u} \rightarrow 4b_{3g}$	$^1B_{2u}$	2.50 (v) [0.0456]	2.95 (v)	2.38 (v)	Q_y (2.42) [0.06]
$4b_{1u} \rightarrow 4b_{2g}$ $5b_{1u} \rightarrow 4b_{2g}$ $2a_u \rightarrow 4b_{3g}$	$^1B_{3u}$	4.40 (v + R) [1.2713]	3.08 (v + R)	3.41 (v)	B_x (3.33) [1.15]
$5b_{1u} \rightarrow 4b_{3g}$ $2a_u \rightarrow 4b_{2g}$	$^1B_{2u}$	4.73 (v) [2.7890]	3.33 (v + R)	3.95 (v + R)	B_y (3.33) [1.15]
$2a_u \rightarrow 5b_{2g}$ •	$^1B_{2u}$	5.07 (R) [0.0337]	3.65 (R)	4.07 (R + v)	N_y (3.65) [< 0.1]
$2a_u \rightarrow 5b_{3g}$ •	$^1B_{3u}$	5.12 (R) [0.0028]	3.44 (R + v)	4.13 (R)	N_x (3.65) [< 0.1]
$5b_{1u} \rightarrow 5b_{2g}$ •	$^1B_{3u}$	5.59 (R) [0.0073]	–	4.31 (R)	L_x (4.25) [≈0.1]
$5b_{1u} \rightarrow 5b_{3g}$ •	$^1B_{2u}$	5.67 (R) [0.0019]	–	4.36 (R)	L_y (4.25) [≈0.1]
$4b_{1u} \rightarrow 4b_{2g}$ $5b_{1u} \rightarrow 4b_{2g}$	$^1B_{3u}$	5.22 (v) [2.2030]	–	4.68 (v + R)	?
$2a_u \rightarrow 6b_{2g}$ • $2a_u \rightarrow 5b_{2g}$ •	$^1B_{2u}$	–	4.39 (R)	4.74 (R)	L_y (4.67) [≈0.1]
$2a_u \rightarrow 6b_{3g}$ •	$^1B_{3u}$	–	4.35 (R)	4.76 (R + v)	L_x (4.67) [≈0.1]
$2a_u \rightarrow 6b_{2g}$ •	$^1B_{2u}$	–	4.53 (R + v)	–	M_y (5.50) [≈0.3]
$2a_u \rightarrow 6b_{3g}$ •	$^1B_{3u}$	–	4.59 (R + v)	–	M_x (5.50) [≈0.3]
$4b_{1u} \rightarrow 4b_{3g}$	$^1B_{2u}$	–	–	4.98 (v)	?

[a] CIS and sa-CASSCF dominant configurations

that the B_x and N_x bands have mixed valence- and Rydberg-type character. The valence-type configuration resulting from the ($4b_{1u} \rightarrow 4b_{2g}$) excitation is found to be a candidate for the series perturber in the $^1B_{3u}$ Rydberg series. Similarly, the configuration resulting from ($5b_{1u} \rightarrow 4b_{3g}$) is a candidate for the perturber in the $^1B_{2u}$ Rydberg series. Although the present study has some qualitative nature owing to the limited number of the Rydberg GTFs and the limitations of the computational methods, the results indicate that the higher electronic absorption spectra of FBP consist of a perturbed Rydberg series.

Since CIS result depends heavily on the MO set and the reference configurations and CASSCF accounts for only a fraction of the electronic correlation effects, a more sophisticated treatment such as MRCISD or MRPT is required in order to obtain reliable values for the excitation energies. We believe, however, that the present results provide useful information for future studies.

Acknowledgements. The present research was supported by a Grant-in-Aid from the Ministry of Education, Culture, Sports, Science and Technology of Japan. S.Y. would like to thank E. W. Schreiner for providing him with detailed explanations concerning the OpenMol CI program and J. Karwowski and W. Duch for leading him to the symmetric group graphical approach. S.Y. also thanks the Alexander von Humboldt Foundation and the Max Planck Institute for Astrophysics for financial support during his stay in Germany.

References

1. Edwards L, Dolphin DH, Gouterman M, Adler AD (1971) J Mol Spectrosc 38: 16
2. Gouterman M (1959) J Chem Phys 30: 1139
3. McHugh AJ, Gouterman M, Weiss C Jr (1972) Theor Chim Acta 24: 346
4. Baker JD, Zerner MC (1990) Chem Phys Lett 175: 192
5. Nagashima U, Takada T, Ohno K (1986) J Chem Phys 85: 4524
6. Yamamoto Y, Noro T, Ohno K (1992) Int J Quantum Chem 42: 1563
7. Foresman JB, Head-Gordon M, Pople JA, Frisch MJ (1992) J Phys Chem 96: 135
8. Yamamoto S, Diercksen GHF, Karelson M (2000) Chem Phys Lett 318: 590
9. Merchán M, Ortí E, Roos BO (1994) Chem Phys Lett 226: 27
10. Serrano-Andrés L, Merchán M, Rubi M, Roos BO (1998) Chem Phys Lett 295: 195
11. Nakatsuji H, Hasegawa J, Hada M (1996) J Chem Phys 104: 2321
12. Hasegawa J, Ozeki Y, Ohkawa K, Hada M, Nakatsuji H (1998) J Phys Chem B 102: 1320
13. Tokita Y, Hasegawa J, Nakatsuji H (1998) J Phys Chem A 102: 1843
14. Kitao O, Ushiyama H, Miura N (1999) J Chem Phys 110: 2936
15. Nooijen M, Bartlett RJ (1997) J Chem Phys 106: 6449
16. Gwaltney SR, Bartlett RJ (1998) J Chem Phys 108: 6790
17. Hashimoto T, Choe Y-K, Nakano H, Hirao K (1999) J Phys Chem A 103: 1894
18. Celani P, Werner H-J (2000) J Chem Phys 112: 5546
19. van Gisbergen SJA, Rosa A, Ricciardi G, Baerends EJ (1999) J Chem Phys 111: 2499
20. Tatewaki H (1978) Phys Rev A 18: 1826
21. Werner H-J (1987) Adv Chem Phys 69: 1
22. Sekino H, Kobayashi H (1981) J Chem Phys 75: 3477
23. Huzinaga S, Andzelm J, Kłobukowski M, Radzio-Andzelm E, Sakai Y, Tatewaki H (1984) Gaussian basis sets for molecular calculations. Elsevier, Amsterdam
24. van Duijneveldt FB (1971) IBM Res Rep RJ945
25. Frisch MJ et al (1998) Gaussian 98, revision A.6. Gaussian, Pittsburgh, Pa, USA
26. Kashiwagi H, Takada T, Miyoshi E, Obara S, Sasaki F (1987) A library program of the Computer Center of the Institute for Molecular Science, Okazaki, Japan
27. Yamamoto S, Nagashima U, Aoyama T, Kashiwagi H (1988) J Comput Chem 9: 627
28. Diercksen GHF, Hall GG (1994) Comput Phys 8: 215; http://www.mpa-garching.mpg.de/∼opmolsrv/OpenMol/home-page.shtml
29. Andersson K et al (1998) MOLCAS, version 4.1. Lund University, Sweden
30. Duch W, Karwowski J (1985) Comput Phys Rep 2: 93
31. Toyota K, Hasegawa J, Nakatsuji H (1996) Chem Phys Lett 250: 437